Julku, Aleksi; Peotta, Sebastiano; Vanhala, Tuomas I.; Kim, Dong Hee; Törmä, Päivi

Geometric Origin of Superfluidity in the Lieb-Lattice Flat Band

Geometric Origin of Superfluidity in the Lieb-Lattice Flat Band

Aleksi Julku,[1] Sebastiano Peotta,[1] Tuomas I. Vanhala,[1] Dong-Hee Kim,[2] and Päivi Törmä[1,*]

[1]*COMP Centre of Excellence, Department of Applied Physics, Aalto University School of Science, FI-00076 Aalto, Finland*
[2]*Department of Physics and Photon Science, School of Physics and Chemistry,*
Gwangju Institute of Science and Technology, Gwangju 61005, Korea

The ground state and transport properties of the Lieb lattice flat band in the presence of an attractive Hubbard interaction are considered. It is shown that the superfluid weight can be large even for an isolated and strictly flat band. Moreover the superfluid weight is proportional to the interaction strength and to the quantum metric, a band structure quantity derived solely from the flat-band Bloch functions. These predictions are amenable to verification with ultracold gases and may explain the anomalous behavior of the superfluid weight of high-T_c superconductors.

A flat band is a Bloch band with constant energy dispersion $\varepsilon_{n\mathbf{k}} \approx \varepsilon_n$ (n is the band index) as a function of quasimomentum $\mathbf{k}$ and is composed of localized eigenstates. In the absence of disorder and interactions the ground state of a flat band is insulating at any filling [1]. However, interactions and disorder lead to a reconstruction of the ground state whose properties are often hard to predict. Bands that are nearly flat and/or feature a nontrivial topological invariant, similar to Landau levels producing the quantum Hall effects [2–4], have been considered in recent theoretical works [5–12] and can be realized in ultracold gas experiments [13–15]. Flat-band ferromagnetism has been studied first by Lieb [16] and, subsequently, by Tasaki and Mielke [17–20]. More recently it has been shown that the high density of states of flat bands enhances the superconducting critical temperature [21,22]. Indeed, for fixed interaction strength, the flat-band dispersion provides the maximal critical temperature within mean-field BCS theory [23].

Flat bands, or quasiflat bands, can be realized in bipartite lattices [16] and other models [6–8,20,24]. A simple bipartite lattice featuring a strictly flat band is the Lieb lattice [Fig. 1(a)]. Recent studies on models defined on the Lieb lattice focus on the ferromagnetic and topological properties [25–31], while superconductivity has been studied in Refs. [28,32]. On the experimental side, a highly tunable Lieb lattice has been realized with ultracold gases [33]. Intriguingly, the CuO_2 planes responsible for the exotic properties of high-T_c cuprate superconductors have the Lieb lattice structure. Thus a Hubbard model on the Lieb lattice [34–36] is a natural, and possibly indispensable [37–39], extension of the single-band Hubbard model more commonly used [40].

The important question of whether an isolated strictly flat band can support superfluid transport is open. Its answer is of interest for ongoing ultracold gas experiments and may have important implications for the theory of superconductivity. The Meissner effect and dissipationless transport are manifestations of a finite superfluid weight that in conventional superconductors at zero temperature reads $D_s = n_p/m_{eff}$, with n_p the particle density and m_{eff} the band effective mass. Interestingly, the superfluid weight of a flat band is not necessarily vanishing, as suggested by $m_{eff} \to +\infty$, but proportional to the quantum metric [41]. Flat bands with nonzero Chern number C (the topological index of Landau levels) have nonzero superfluid weight due to the bound $D_s \geq |C|$. For a large class of Hamiltonians defined on the Lieb lattice the flat band has $C = 0$ [42]. Lower bounds on D_s are not available at present for topologically trivial bands or bands characterized by other topological invariants than the Chern number.
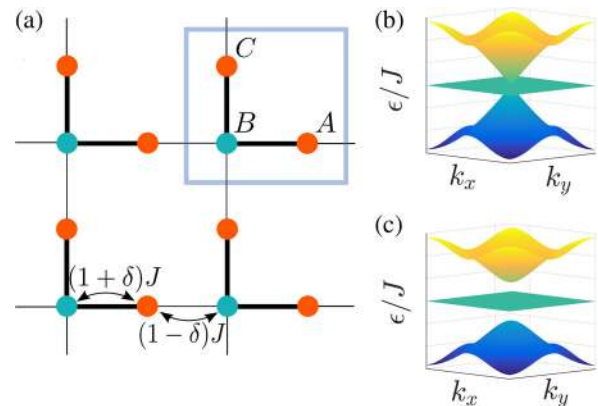
FIG. 1. (a) The Lieb lattice and its unit cell (gray box) are shown. The orbitals in the unit cell are labeled by $\alpha = A, B, C$. The thick lines represent nearest-neighbor hoppings with energy $(1 + \delta)J$, while the hopping energy corresponding to the thin lines is $(1 - \delta)J$ with $0 \leq \delta \leq 1$ parametrizing the staggered hopping. (b)–(c) The energy dispersion as a function of quasimomentum $\mathbf{k}$ for $\delta = 0$ (b) and $\delta = 0.3$ (c), respectively. The middle band is strictly flat $\varepsilon_{0\mathbf{k}} = 0$ for any value of δ while the upper and lower band have dispersions $\varepsilon_{\pm,\mathbf{k}} = \pm 2J\sqrt{1 + \delta^2 + (1 - \delta^2)(\cos k_x a + \cos k_y a)/2}$.

Here we consider a tight-binding model with attractive Hubbard interaction on the Lieb lattice. This model features a strictly flat band with $C = 0$. We show that the total superfluid weight tensor receives contributions from the flat band, $D_s|_{\text{f.b.}}$, and from the other bands, $D_s|_{\text{o.b.}}$, that is, $D_s = D_s|_{\text{f.b.}} + D_s|_{\text{o.b.}}$. We find that $D_s|_{\text{f.b.}}$ depends on the flat-band Bloch functions through the quantum metric. This is called a "geometric" contribution distinct from the "conventional" contribution, which depends only on the derivatives of $\varepsilon_{n\mathbf{k}}$ [41]. Only the latter is accounted for when evaluating the superfluid weight of known superconductors [43,44]. Importantly, the energy scale of the geometric contribution is the coupling constant U, at odds with the conventional result $D_s = n_p/m_{\text{eff}} \propto J$, where J is the characteristic hopping energy in a tight-binding Hamiltonian. We identify the regimes where $D_s|_{\text{f.b.}}$ dominates over the term $D_s|_{\text{o.b.}}$, which includes the conventional and geometric contributions of other bands. These results are obtained with mean-field BCS theory. The validity of BCS theory is rigorously justified by showing that, in the isolated flat-band limit, the BCS wave function is exact for any bipartite lattice. Furthermore, we compare the BCS predictions for the pairing order parameters and the superfluid weight, respectively, with dynamical mean-field theory (DMFT) and exact diagonalization (ED), finding good agreement even when the flat band is not isolated.

Hubbard model on the Lieb lattice.—The Hamiltonian $\hat{\mathcal{H}} = \hat{\mathcal{H}}_{\text{kin}} + \hat{\mathcal{H}}_{\text{int}} - \mu\hat{N}$ defined on the Lieb lattice comprises the chemical potential term $-\mu\hat{N}$ ($\hat{N}$ is the particle number operator), the attractive Hubbard interaction $\hat{\mathcal{H}}_{\text{int}}$ defined below and the kinetic term $\hat{\mathcal{H}}_{\text{kin}} = \sum_{\mathbf{k},\sigma} \hat{\mathbf{c}}_{\mathbf{k}\sigma}^{\dagger} H_{\mathbf{k}} \hat{\mathbf{c}}_{\mathbf{k}\sigma}$ with staggered nearest-neighbor hopping [Fig. 1(a)]

$$H_{\mathbf{k}} = 2J \begin{pmatrix} 0 & a_{\mathbf{k}} & 0 \\ a_{\mathbf{k}}^* & 0 & b_{\mathbf{k}} \\ 0 & b_{\mathbf{k}}^* & 0 \end{pmatrix}, \qquad (1)$$

where $a_{\mathbf{k}} = \cos(k_x a/2) + i\delta\sin(k_x a/2)$, $b_{\mathbf{k}} = \cos(k_y a/2) + i\delta\sin(k_y a/2)$, and a is the lattice constant. The fermion operators are defined as $\hat{\mathbf{c}}_{\mathbf{k}\sigma} = (\hat{c}_{A\mathbf{k}\sigma}, \hat{c}_{B\mathbf{k}\sigma}, \hat{c}_{C\mathbf{k}\sigma})^T$ and $\hat{c}_{\alpha\mathbf{k}\sigma} = (1/\sqrt{N_c})\sum_{\mathbf{i}} e^{-i\mathbf{k}\cdot\mathbf{r}_{\mathbf{i}\alpha}} \hat{c}_{\mathbf{i}\alpha\sigma}$, where N_c is the number of unit cells, $\mathbf{r}_{\mathbf{i}\alpha}$ is the position vector of the α orbital in the $\mathbf{i}$th unit cell [$\mathbf{i} = (i_x, i_y)^T$], and the operator $\hat{c}_{\mathbf{i}\alpha\sigma}$ annihilates a fermion with spin $\sigma = \uparrow, \downarrow$ in the orbital centered at $\mathbf{r}_{\mathbf{i}\alpha}$. By solving the eigenvalue problem $H_{\mathbf{k}}|g_{n\mathbf{k}}\rangle = \varepsilon_{n\mathbf{k}}|g_{n\mathbf{k}}\rangle$ one obtains the Bloch functions $|g_{n\mathbf{k}}\rangle$ and the band dispersions $\varepsilon_{n\mathbf{k}}$ ($n = 0, \pm$). The middle band is strictly flat ($\varepsilon_{n=0,\mathbf{k}} = 0$) for any value of the staggered-hopping parameter δ and isolated from the other bands by an energy gap $E_{\text{gap}} = \sqrt{8}J\delta$. The Hubbard interaction $\hat{\mathcal{H}}_{\text{int}} = -U\sum_{\mathbf{i},\alpha}(\hat{n}_{\mathbf{i}\alpha\uparrow} - 1/2)(\hat{n}_{\mathbf{i}\alpha\downarrow} - 1/2)$, where $U > 0$ and $\hat{n}_{\mathbf{i}\alpha\sigma} = \hat{c}_{\mathbf{i}\alpha\sigma}^{\dagger}\hat{c}_{\mathbf{i}\alpha\sigma}$, is approximated by mean-field pairing $\Delta_{\alpha} = -U\langle\hat{c}_{\mathbf{i}\alpha\downarrow}\hat{c}_{\mathbf{i}\alpha\uparrow}\rangle$ and Hartree potentials $n_{\alpha} = \langle\hat{n}_{\mathbf{i}\alpha\sigma}\rangle$

$$\hat{\mathcal{H}}_{\text{int}} \approx \sum_{\mathbf{i},\alpha} (\Delta_{\alpha}\hat{c}_{\mathbf{i}\alpha\uparrow}^{\dagger}\hat{c}_{\mathbf{i}\alpha\downarrow}^{\dagger} + \text{H.c.}) + U\sum_{\mathbf{i},\alpha,\sigma}\left(n_{\alpha} - \frac{1}{2}\right)\hat{n}_{\mathbf{i}\alpha\sigma}. \quad (2)$$

The equivalence of orbitals A and C implies $\Delta_A = \Delta_C$ and $n_A = n_C$. From the zero-temperature gap equations at half filling $\nu = \sum_{\alpha}n_{\alpha} = 3/2$ one finds $\Delta_A = U/4$ and $\Delta_B = 0$ at leading order in U/J [45].

Exactness of BCS wave function for a flat band.—The Lieb theorem [16] states that the ground state at half filling of a bipartite lattice with repulsive Hubbard interaction has total spin $S = N_c N_{\text{f.b.}}/2$, where $N_{\text{f.b.}}$ is the number of flat bands and N_c the number unit cells. The Lieb lattice has $N_{\text{f.b.}} = 1$ and if $U \ll E_{\text{gap}}$, the completely filled lower band can be neglected at half filling. The ferromagnetic wave functions $|\text{Ferro}\rangle = \prod_{\mathbf{k}}(ud_{0\mathbf{k}\downarrow}^{\dagger} + vd_{0\mathbf{k}\uparrow}^{\dagger})|\emptyset\rangle$, parametrized by u, v with $|u|^2 + |v|^2 = 1$, have total spin S and therefore are the only ground states. Here the operator $d_{n=0,\mathbf{k}\sigma}^{\dagger}$ creates a fermion within the flat band. A repulsive Hubbard model on a bipartite lattice can be mapped by a particle-hole transformation into an attractive one [51]. Under this transformation the state $|\text{Ferro}\rangle$ is mapped into a BCS wave function $|\text{BCS}\rangle = \prod_{\mathbf{k}}(u + vd_{0\mathbf{k}\uparrow}^{\dagger}d_{0(-\mathbf{k})\downarrow}^{\dagger})|\emptyset\rangle$ and the spin operator along the z axis $\hat{S}_{\mathbf{i}\alpha}^z = \frac{1}{2}(\hat{n}_{\mathbf{i}\alpha\uparrow} - \hat{n}_{\mathbf{i}\alpha\downarrow})$ into the operator $\hat{\Delta}_{\mathbf{i}\alpha}^z = \frac{1}{2}(\hat{n}_{\mathbf{i}\alpha\uparrow} + \hat{n}_{\mathbf{i}\alpha\downarrow} - 1)$. The expectation value $\langle\sum_{\alpha}\hat{\Delta}_{\mathbf{i}\alpha}^z\rangle = \nu - 3/2$ gives the filling ν. Therefore, the BCS wave function is the exact ground state for arbitrary flat band filling. This result is easily extended to any bipartite lattice. Consistently with this result, the numerical data obtained with DMFT and ED converge to the predictions of BCS theory for small U and a partially filled flat band, as we show below and in Ref. [45].

Comparison with DMFT.—To investigate the accuracy of BCS theory also for a nonisolated flat band, we compare it in Fig. 2 against DMFT with respect to the pairing potentials (order parameters) Δ_A [Fig. 2(a)] and Δ_B [Fig. 2(b)] as a function of δ at half filling. We use cellular dynamical mean-field theory [52,53] with a continuous-time interaction-expansion impurity solver [54,55], which
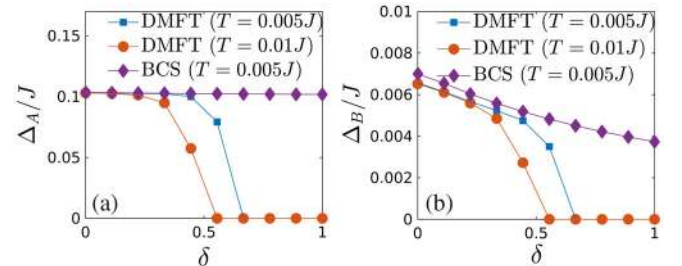

FIG. 2. Order parameters Δ_A/J (left) and Δ_B/J (right) as a function of δ obtained with DMFT and mean-field BCS theory at temperatures $k_B T = 5 \times 10^{-3}$ and $10^{-2} J$, filling $\nu = 1.5$ and coupling strength $U = 0.4 J$. At these temperatures, significantly lower than the BCS critical temperature $k_B T_{c,\text{BCS}} \approx \Delta_A/2 = U/8 = 5 \times 10^{-2} J$, the BCS results are indistinguishable from the zero temperatures ones.
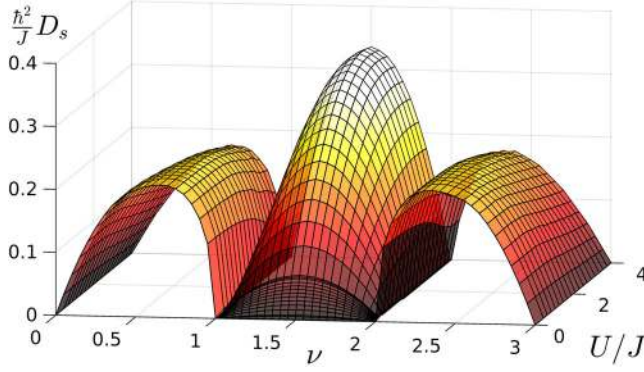
FIG. 3.   Diagonal components of the superfluid weight tensor $[D_s]_{x,x} = [D_s]_{y,y} \approx D_s$ as a function of interaction U/J and filling ν for $\delta = 10^{-3}$ and at zero temperature. The superfluid weight for partially filled flat band ($1 \leq \nu \leq 2$) depends strongly on U in contrast to the other bands.

treats correlations exactly within the three-site unit cell and goes beyond mean-field BCS theory. For small δ, DMFT is in good agreement with BCS, especially regarding Δ_A. The results for large δ are discussed below. In particular, both methods show that, even when $\delta = E_{\text{gap}} = 0$, pairing is dominated by the flat band and the effect of the other bands is small.

Superfluid weight.—The superfluid weight is defined as the change in free energy density $\Delta f = \frac{1}{8} D_s (\hbar q)^2$ due to the winding with wave vector **q** of the order parameter phase $\Delta(\mathbf{r}) = \Delta e^{2i\mathbf{q}\cdot\mathbf{r}}$. The superfluid weight obtained from multiband BCS theory is shown in Fig. 3 as a function of coupling U and filling ν for zero temperature and $\delta = 10^{-3}$ [45]. The Hartree term of Eq. (2) is needed for preserving the $SU(2)$ symmetry that allows us to calculate D_s for arbitrary flat band fillings [32]. This symmetry corresponds, under the particle-hole transformation, to the spin rotational symmetry of the repulsive Hubbard model. For $\delta \neq 0$, the superfluid weight tensor acquires nonzero off-diagonal components $[D_s]_{x,y} = [D_s]_{y,x}$. However, this effect is small and we focus only on the diagonal components $[D_s]_{x,x} = [D_s]_{y,y} \approx D_s$.

A striking feature of Fig. 3 is that, for partially filled dispersive bands, D_s is finite and roughly constant as a function of U, while the superfluid weight within the flat band depends strongly on U and has a nonmonotonic behavior [see also Fig. 4(a)]. This is consistent with the fact that superconductivity in the dispersive bands emerges from a metallic state with nonzero Drude weight which is the $U \to 0$ limit of D_s at zero temperature [56,57]. On the contrary, superconductivity in the flat band smoothly emerges with increasing U from an insulating state with zero Drude weight. Notably, the superfluid weight of a topologically trivial flat band can be nonzero and larger than the one of dispersive bands in the same model.

This peculiar behavior is a consequence of the geometric origin of flat-band superfluidity. The total superfluid weight can be split in conventional and geometric contributions $D_s = D_{s,\text{conv}} + D_{s,\text{geom}}$. The conventional contribution $D_{s,\text{conv}} \propto J$ depends only on the derivatives of the dispersions $\varepsilon_{n\mathbf{k}}$ while the geometric one $D_{s,\text{geom}} \propto \Delta_A$ includes derivatives of the Bloch functions $|g_{n\mathbf{k}}\rangle$ [45]. Obviously the flat band does not contribute to the conventional term, while $D_{s,\text{geom}} = D_{s,\text{geom}}|_{\text{f.b.}} + D_{s,\text{geom}}|_{\text{o.b.}}$ can be further split into a term originating purely from the flat band $D_{s,\text{geom}}|_{\text{f.b.}} = D_s|_{\text{f.b.}}$ and the remaining part $D_{s,\text{geom}}|_{\text{o.b.}}$, which includes the geometric effect of the other bands. All three terms $D_{s,\text{conv}}, D_{s,\text{geom}}|_{\text{f.b.}}$ and $D_{s,\text{geom}}|_{\text{o.b.}}$ are invariant with respect to the gauge freedom consisting in the multiplication of the Bloch functions by an arbitrary **k**-dependent phase factor and are thus well defined. In our model the flat-band term $D_s|_{\text{f.b.}}$ at half filling has the form

$$[D_s]_{i,j}|_{\text{f.b.}} = \frac{4}{\pi\hbar^2}\frac{\Delta_A^2}{U}\mathcal{M}_{ij}^R|_{\text{f.b.}} \approx \frac{U}{4\pi\hbar^2}\mathcal{M}_{ij}^R|_{\text{f.b.}}, \quad (3)$$

where $\mathcal{M}_{ij}^R|_{\text{f.b.}} = (2\pi)^{-1}\int_{\text{B.Z.}} d^2\mathbf{k}\,\text{Re}\mathcal{B}_{ij}(\mathbf{k})|_{\text{f.b.}}$ is the Brillouin-zone integral of the flat-band quantum metric $\text{Re}\mathcal{B}_{ij}(\mathbf{k})|_{\text{f.b.}}$. The quantum metric is defined as the real part of the quantum geometric tensor [1,58,59]

$$\mathcal{B}_{ij}(\mathbf{k})|_{\text{f.b.}} = 2\langle\partial_{k_i}g_{0\mathbf{k}}|(1 - |g_{0\mathbf{k}}\rangle\langle g_{0\mathbf{k}}|)|\partial_{k_j}g_{0\mathbf{k}}\rangle. \quad (4)$$
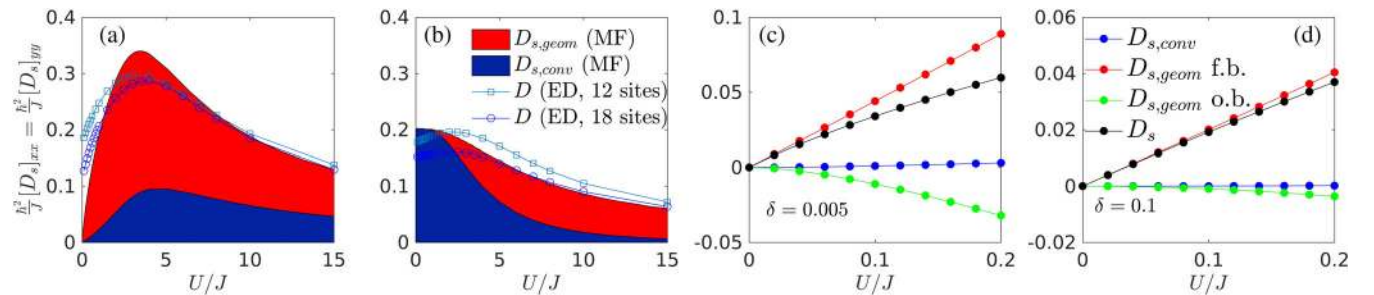

FIG. 4.   (a)–(b) Conventional superfluid weight $D_{s,\text{conv}}$ (blue area) compared with the geometric one $D_{s,\text{geom}}$ (red area) for $\nu = 1.5$ (a) and $\nu = 2.5$ (b). Here $T = 0$ and $\delta = 10^{-3}$. Also the Drude weight D obtained from ED is shown. Squares and circles correspond to the 12 sites and 18 sites clusters, respectively. Data for the 24 sites cluster at $\nu = 2.5$ (shown in Ref. [45]) do not deviate significantly with respect to 18 sites. (c)–(d) Various superfluid weight contributions for half-filled flat band, small $U \leq 0.2\,J$, $\delta = 5 \times 10^{-3}$ (c), $\delta = 0.1$ (d).

The same quantity $\mathcal{M}^R$ appears in the theory of the polarization [1,60] and current [61] fluctuations in band insulators.

The strong dependence of D_s on U for a partially filled flat band originates from the geometric term as shown in Figs. 4(a)–4(b), where $D_{s,\text{conv}}$ and $D_{s,\text{geom}}$ are presented as a function of U for half-filled flat band [$\nu = 1.5$, Fig. 4(a)] and half-filled upper band [$\nu = 2.5$, Fig. 4(b)]. For $\nu = 1.5$ the term $D_{s,\text{geom}}$ dominates $D_{s,\text{conv}}$, while for $\nu = 2.5$ $D_{s,\text{geom}}$ is negligible at weak coupling.

In order to confirm the behavior of D_s observed in the mean-field calculations, we compute the Drude weight D by using ED on periodic finite-size clusters of 12, 18, and 24 sites [45,62]. In the bulk limit D is equivalent to D_s for gapped systems [56,57,63]. Figures 4(a)–4(b) show that D_s from BCS theory is in good agreement with ED results. In particular, at half filling ($\nu = 1.5$), the sharp increase of D for $0 \le U \lesssim 4\,J$ becomes clearer with increasing cluster size. It is also peaked at $U \sim 4\,J$ and decreases when U further increases, confirming the overall behavior of the mean-field D_s. The drastic difference between $\nu = 1.5$ and 2.5, namely, D_s approaching zero vs being a finite constant, respectively, in the small U limit is also confirmed by ED. The finite D for $\nu = 2.5$ at small coupling shows very weak dependence on U for cluster size up to 24 sites.

Note that D_s scales in a way similar to the pair structure factor P_s obtained in Ref. [32] with determinant quantum Monte Carlo calculations. At fixed $U = 4\,J$ the values $P_s \sim 0.1$ and $P_s \sim 0.05$ for $\nu = 1.5$ and $\nu = 2.5$, respectively, can be compared to our results $D_s \sim 0.33\,J/\hbar^2$ and $D_s \sim 0.16\,J/\hbar^2$. Furthermore at fixed $\nu = 1.5$ the values $P_s \sim 0.10$ ($U = 4\,J$) and $P_s \sim 0.07$ ($U = 8\,J$) correspond to $D_s \sim 0.33\,J/\hbar^2$ and $D_s \sim 0.23\,J/\hbar^2$, respectively.

In Figs. 4(c)–4(d) we compare the conventional term $D_{s,\text{conv}}$, the flat-band contribution $D_s|_{\text{f.b.}}$ and the geometric contribution due to the other bands $D_{s,\text{geom}}|_{\text{o.b.}}$ at half filling $\nu = 1.5$ and for small $U \le 0.2\,J$. Two values of δ are shown: $\delta = 5 \times 10^{-3}$ [Fig. 4(c)] and $\delta = 0.1$ [Fig. 4(d)]. In both cases $D_{s,\text{conv}}$ is negligible due to the vanishing density of states of the dispersive bands, while $D_s|_{\text{f.b.}}$ gives the dominant contribution, linear in U. The term $D_{s,\text{geom}}|_{\text{o.b.}}$ is negative and less relevant when the flat band becomes more isolated for larger δ. When U increases, the negative contribution of $D_{s,\text{geom}}|_{\text{o.b.}}$ becomes more prominent and for very large U it cancels the positive term $D_s|_{\text{f.b.}}$ [see Fig. 4(a)]. This means that pairing has to occur in a subset of all bands for $D_{s,\text{geom}}$ to manifest, and it explains the decreasing trend of D_s in Figs. 4(a)–4(b). As shown in Fig. 5, the invariant $\mathcal{M}^R_{ij}|_{\text{f.b.}}$ diverges at $\delta = 0$; thus, the slope of D_s as a function of U is infinite at $U = 0$. However for any nonzero U we have verified that this divergence is cured by $D_{s,\text{geom}}|_{\text{o.b.}}$. Thus, for $\delta = 0$ superfluidity has a truly multiband character. In the opposite limit $\delta \to 1$ one eigenvalue of $\mathcal{M}^R_{ij}|_{\text{f.b.}}$ becomes zero and superfluidity is lost, consistently with the fact that the unit cells become
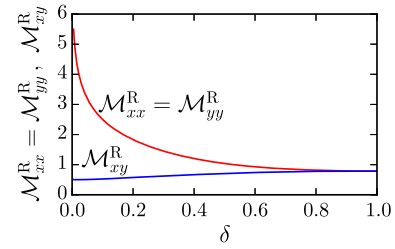
FIG. 5. Brillouin-zone integral of the flat-band quantum metric $\mathcal{M}^R_{ij}|_{\text{f.b.}}$ as a function of δ. The diagonal components have a logarithmic singularity at $\delta = 0$.

decoupled [see Fig. 1(a)]. In contrast to mean-field theory, DMFT captures this behavior already at the level of the order parameter, as seen in Fig. 2.

Discussion.—The main result of this work is that topologically trivial flat bands are promising for high-T_c superconductivity, in the same way as topologically non-trivial ones. Indeed, a flat band allows us to optimize not only the BCS critical temperature [23], but also the superfluid weight [see Figs. 4(a)–4(b)]. The superfluid weight affects the critical temperature in two dimensions through the Berezinsky-Kosterlitz-Thouless (BKT) transition. We show that the superfluid weight has geometric origin; i.e., it is proportional to the quantum metric of the flat band [Eqs. (3)–(4)]. The fingerprint of the geometric origin is the strong dependence of D_s on the coupling constant U, possibly observable in ultracold gases where interactions are tunable.

Achieving the superfluid phase of an ultracold gas in an optical lattice is difficult, due to the still too high temperatures (specific entropies) currently attainable [64,65]. We find the BKT transition temperature in the Lieb lattice to be $k_B T_{c,\text{BKT}} = \pi \hbar^2 D_s(T_{c,\text{BKT}})/8 = 0.133\,J$ [45] at the optimal coupling $U \approx 4\,J$ [Fig. 4(a)], to be compared with the quantum Monte Carlo estimate $k_B T_{c,\text{BKT}} \sim 0.10$–$0.13\,J$ at $U = 4\,J$ for the 2D simple square lattice [66] (for three dimensions see Ref. [67]). Therefore lattices with flat bands whose integrated quantum metric $\mathcal{M}^R$ is large are a promising path to achieve higher critical temperature in ultracold gases.

In the solid state context the geometric contribution to the superfluid weight is expected to be larger for superconductors with high T_c and provides a possible explanation of the linear relation between superfluid weight and critical temperature in cuprates (Uemura relation [68,69]) since $D_{s,\text{geom}} \propto \Delta \propto T_c$. We expect $D_{s,\text{geom}}$ to be significant in models with nontrivial Bloch functions also with the different pairing symmetries found in high-T_c superconductors, whose incorporation to our theory for the superfluid weight is an important topic of future research.

PHYSICAL REVIEW LETTERS

---

*paivi.torma@aalto.fi

[1] R. Resta, The insulating state of matter: a geometrical theory, Eur. Phys. J. B **79,** 121 (2011).

[2] *The Quantum Hall Effect*, 2nd ed., edited by R. E. Prange and S. M. Girvin (Springer-Verlag, New York, 1990).

[3] *The Quantum Hall Effect*, 2nd ed., edited by T. Chakraborty and P. Pietiläinen (Springer-Verlag, Berlin-Heidelberg, 1995).

[4] *Perspectives in Quantum Hall Effects: Novel Quantum Liquids in Low Dimensional Semiconductor Structures*, edited by S. das Sarma and A. Pinczuk (Wiley-VCH Verlag, New York, 2004).

[5] S. D. Huber and E. Altman, Bose condensation in flat bands, Phys. Rev. B **82,** 184502 (2010).

[6] K. Sun, Z. Gu, H. Katsura, and S. Das Sarma, Nearly Flatbands with Nontrivial Topology, Phys. Rev. Lett. **106,** 236803 (2011).

[7] E. Tang, J.-W. Mei, and X.-G. Wen, High-Temperature Fractional Quantum Hall States, Phys. Rev. Lett. **106,** 236802 (2011).

[8] T. Neupert, L. Santos, C. Chamon, and C. Mudry, Fractional Quantum Hall States at Zero Magnetic Field, Phys. Rev. Lett. **106,** 236804 (2011).

[9] E. J. Bregholtz and Z. Liu, Topological flat band models and fractional Chern insulators, Int. J. Mod. Phys. B **27,** 1330017 (2013).

[10] R. Roy, Band geometry of fractional topological insulators, Phys. Rev. B **90,** 165139 (2014).

[11] S. Takayoshi, H. Katsura, N. Watanabe, and H. Aoki, Phase diagram and pair Tomonaga-Luttinger liquid in a Bose-Hubbard model with flat bands, Phys. Rev. A **88,** 063613 (2013).

[12] M. Tovmasyan, E. P. L. van Nieuwenburg, and S. D. Huber, Geometry-induced pair condensation, Phys. Rev. B **88,** 220510 (2013).

[13] M. Aidelsburger, M. Atala, M. Lohse, J. T. Barreiro, B. Paredes, and I. Bloch, Realization of the Hofstadter Hamiltonian with Ultracold Atoms in Optical Lattices, Phys. Rev. Lett. **111,** 185301 (2013).

[14] H. Miyake, G. A. Siviloglou, C. J. Kennedy, W. C. Burton, and W. Ketterle, Realizing the Harper Hamiltonian with Laser-Assisted Tunneling in Optical Lattices, Phys. Rev. Lett. **111,** 185302 (2013).

[15] M. Aidelsburger, M. Lohse, C. Schweizer, M. Atala, J. T. Barreiro, S. Nascimbène, N. R. Cooper, I. Bloch, and N. Goldman, Measuring the Chern number of Hofstadter bands with ultracold bosonic atoms, Nat. Phys. **11,** 162 (2015).

[16] E. H. Lieb, Two Theorems on the Hubbard Model, Phys. Rev. Lett. **62,** 1201 (1989).

[17] A. Mielke, Ferromagnetic ground states for the Hubbard model on line graphs, J. Phys. A **24,** L73 (1991); Ferromagnetism in the Hubbard model on line graphs and further considerations, J. Phys. A **24,** 3311 (1991).

[18] H. Tasaki, Ferromagnetism in the Hubbard models with degenerate single-electron ground states, Phys. Rev. Lett. **69,** 1608 (1992).

[19] A. Mielke and H. Tasaki, Ferromagnetism in the Hubbard model, Commun. Math. Phys. **158,** 341 (1993).

[20] H. Tasaki, From Nagaoka's ferromagnetism to flat-band ferromagnetism and beyond, Prog. Theor. Phys. **99,** 489 (1998).

[21] N. B. Kopnin, T. T. Heikkilä, and G. E. Volovik, High-temperature surface superconductivity in topological flat-band systems, Phys. Rev. B **83,** 220503(R) (2011).

[22] T. T. Heikkilä, N. B. Kopnin, and G. E. Volovik, Flat bands in topological media, JETP Lett. **94,** 233 (2011).

[23] K. Noda, K. Inaba, and M. Yamashita, BCS superconducting transitions in lattice fermions, arXiv:1512.07858.

[24] C. Weeks and M. Franz, Topological insulators on the Lieb and perovskite lattices, Phys. Rev. B **82,** 085310 (2010).

[25] K. Noda, A. Koga, N. Kawakami, and T. Pruschke, Ferromagnetism of cold fermions loaded into a decorated square lattice, Phys. Rev. A **80,** 063622 (2009).

[26] N. Goldman, D. F. Urban, and D. Bercioux, Topological phases for fermionic cold atoms on the Lieb lattice, Phys. Rev. A **83,** 063601 (2011).

[27] K. Noda, K. Inaba, and M. Yamashita, Flat-band ferromagnetism in the multilayer Lieb optical lattice, Phys. Rev. A **90,** 043624 (2014).

[28] K. Noda, K. Inaba, and M. Yamashita, Magnetism in the three-dimensional layered Lieb lattice: Enhanced transition temperature via flat-band and Van Hove singularities, Phys. Rev. A **91,** 063610 (2015).

[29] W.-F. Tsai, C. Fang, H. Yao, and J. Hu, Interaction-driven topological and nematic phases on the Lieb lattice, New J. Phys. **17,** 055016 (2015).

[30] G. Palumbo and K. Meichanetzidis, Two-dimensional Chern semimetals on the Lieb lattice, Phys. Rev. B **92,** 235106 (2015).

[31] A. Dauphin, M. Müller, and M. A. Martin-Delgado, Quantum simulation of a topological Mott insulator with Rydberg atoms in a Lieb lattice, Phys. Rev. A **93,** 043611 (2016).

[32] V. I. Iglovikov, F. Hébert, B. Grémaud, G. G. Batrouni, and R. T. Scalettar, Superconducting transitions in flat-band systems, Phys. Rev. B **90,** 094506 (2014).

[33] S. Taie, H. Ozawa, T. Ichinose, T. Nishio, S. Nakajima, and Y. Takahashi, Coherent driving and freezing of bosonic matter wave in an optical Lieb lattice, Sci. Adv. **1,** e1500854 (2015).

[34] L. F. Mattheiss, Electronic band properties and superconductivity in $La_{2-y}X_yCuO_4$, Phys. Rev. Lett. **58,** 1028 (1987).

[35] C. M. Varma, S. Schmitt-Rink, and E. Abrahams, Charge transfer excitations and superconductivity in "ionic", metals, Solid State Commun. **62**, 681 (1987).

[36] V. J. Emery, Theory of High-T_c Superconductivity in Oxides, Phys. Rev. Lett. **58**, 2794 (1987).

[37] Y. F. Kung, C.-C. Chen, Y. Wang, E. W. Huang, E. A. Nowadnick, B. Moritz, R. T. Scalettar, S. Johnston, and T. P. Devereaux, Characterizing the three-orbital Hubbard model with determinant quantum Monte Carlo, Phys. Rev. B **93**, 155166 (2016).

[38] V. V. Val'kov, D. M. Dzebisashvili, M. M. Korovushkin, and A. F. Barabanov, Stability of the superconducting $d_{x^2-y^2}$-wave pairing towards the intersite Coulomb repulsion between oxygen holes in high-Tc superconductors, JETP Lett. **103**, 385 (2016).

[39] C. P. J. Adolphs, S. Moser, G. A. Sawatzky, and M. Berciu, Non-Zhang-Rice Singlet Character of the First Ionization State of T-CuO, Phys. Rev. Lett. **116**, 087002 (2016).

[40] J. P. F. LeBlanc et al., Solutions of the Two-Dimensional Hubbard Model: Benchmarks and Results from a Wide Range of Numerical Algorithms, Phys. Rev. X **5**, 041041 (2015).

[41] S. Peotta and P. Törmä, Superfluidity in topologically nontrivial flat bands, Nat. Commun. **6**, 8944 (2015).

[42] L. Chen, T. Mazaheri, A. Seidel, and X. Tang, The impossibility of exactly flat non-trivial Chern bands in strictly local periodic tight binding models, J. Phys. A **47**, 152001 (2014).

[43] R. Prozorov and R. Giannetta, Magnetic penetration depth in unconventional superconductors, Supercond. Sci. Technol. **19**, R41 (2006).

[44] R. Prozorov and V. G. Kogan, London penetration depth in iron-based superconductors, Rep. Prog. Phys. **74**, 124505 (2011).

[45] See Supplemental Material at http://link.aps.org/supplemental/10.1103/PhysRevLett.117.045303, which includes Refs. [46–50]. We provide more details and analytical results on the mean-field theory used for obtaining the superfluid weight. Furthermore, we discuss in detail the argument showing that the BCS wave function is an exact ground state in a flat band and provide additional DMFT data and the estimate of the BKT critical temperature. Also, the detailed settings of the ED calculations are provided.

[46] G. Grosso and G. P. Parravicini, Solid State Physics, 2nd ed. (Elsevier, New York, 2014).

[47] E. H. Lieb, M. Loss, and R. J. McCann, Uniform density theorem for the Hubbard model, J. Math. Phys. **34**, 891 (1993).

[48] A. Georges and G. Kotliar, and W. Krauth, and M. J. Rozenberg, Dynamical mean-field theory of strongly correlated fermion systems and the limit of infinite dimensions, Rev. Mod. Phys. **68**, 13 (1996).

[49] G. Kotliar, S. Y. Savrasov, G. Pálsson, and G. Biroli, Cellular Dynamical Mean Field Approach to Strongly Correlated Systems, Phys. Rev. Lett. **87**, 186401 (2001).

[50] D. R. Nelson and J. M. Kosterlitz, Universal Jump in the Superfluid Density of Two-Dimensional Superfluids, Phys. Rev. Lett. **39**, 1201 (1977).

[51] V. J. Emery, Theory of the quasi-one-dimensional electron gas with strong "on-site" interactions, Phys. Rev. B **14**, 2989 (1976).

[52] T. Maier, M. Jarrell, T. Pruschke, and M. H. Hettler, Quantum cluster theories, Rev. Mod. Phys. **77**, 1027 (2005).

[53] T. I. Vanhala, J. E. Baarsma, M. O. J. Heikkinen, M. Troyer, A. Harju, and P. Törmä, Superfluidity and density order in a bilayer extended Hubbard model, Phys. Rev. B **91**, 144510 (2015).

[54] A. N. Rubtsov, V. V. Savkin, and A. I. Lichtenstein, Continuous-time quantum Monte Carlo method for fermions, Phys. Rev. B **72**, 035122 (2005).

[55] E. Gull, A. J. Millis, A. I. Lichtenstein, A. N. Rubtsov, M. Troyer, and P. Werner, Continuous-time Monte Carlo methods for quantum impurity models, Rev. Mod. Phys. **83**, 349 (2011).

[56] D. J. Scalapino, S. R. White, and S.-C. Zhang, Superfluid density and the Drude weight of the Hubbard model, Phys. Rev. Lett. **68**, 2830 (1992).

[57] D. J. Scalapino, S. R. White, and S.-C. Zhang, Insulator, metal, or superconductor: the criteria, Phys. Rev. B **47**, 7995 (1993).

[58] J. P. Provost and G. Vallee, Riemannian structure on manifolds of quantum states, Commun. Math. Phys. **76**, 289 (1980).

[59] M. V. Berry, The quantum phase, five years after, in Geometric Phases in Physics, edited by A. Shapere and F. Wilczeck (World Scientific, Singapore, 1989), p. 7.

[60] I. Souza, T. Wilkens, and R. M. Martin, Polarization and localization in insulators: Generating function approach, Phys. Rev. B **62**, 1666 (2000).

[61] T. Neupert, C. Chamon, and C. Mudry, Measuring the quantum geometry of Bloch bands with current noise, Phys. Rev. B **87**, 245103 (2013).

[62] E. Dagotto, A. Moreo, F. Ortolani, J. Riera, and D. J. Scalapino, Optical conductivity of the two-dimensional Hubbard model, Phys. Rev. B **45**, 10107 (1992).

[63] P. J. H. Denteneer, Superfluid density in the two-dimensional attractive Hubbard model: quantitative estimates, Phys. Rev. B **49**, 6364 (1994).

[64] T. Esslinger, Fermi-Hubbard Physics with atoms in an optical Lattice, Annu. Rev. Condens. Mater. Phys. **1**, 129 (2010).

[65] R. Jördens et al., Quantitative Determination of Temperature in the Approach to Magnetic Order of Ultracold Fermions in an Optical Lattice, Phys. Rev. Lett. **104**, 180401 (2010).

[66] T. Paiva, R. R. dos Santos, R. T. Scalettar, and P. J. H. Denteneer, Critical temperature for the two-dimensional attractive Hubbard model, Phys. Rev. B **69**, 184501 (2004).

[67] S. Fuchs, E. Gull, L. Pollet, E. Burovski, E. Kozik, T. Pruschke, and M. Troyer, Thermodynamics of the 3D Hubbard Model on Approaching the Néel Transition, Phys. Rev. Lett. **106**, 030401 (2011).

[68] Y. J. Uemura et al., Universal Correlations between T_c and n_s/m^* (carrier density over effective mass) in High-T_c Cuprate Superconductors, Phys. Rev. Lett. **62**, 2317 (1989).

[69] P. A. Marchetti and G. Bighin, Gauge approach to superfluid density in underdoped cuprates, Europhys. Lett. **110**, 37001 (2015), and references therein.